

A non-perturbative analysis of symmetry breaking in two-dimensional 4 theory using periodic field methods

Pablo J. M. Arrero^y, Erick A. Roura^z, and Dean Lee^x

Department of Physics and Astronomy
University of Massachusetts, Amherst, MA 01003

February 1, 2020

Abstract

We describe the generalization of spherical field theory to other modal expansion methods. The main approach remains the same, to reduce a d -dimensional field theory into a set of coupled one-dimensional systems. The method we discuss here uses an expansion with respect to periodic-box modes. We apply the method to 4 theory in two dimensions and compute the critical coupling and critical exponents. We compare with lattice results and predictions via universality and the two-dimensional Ising model. PACS numbers: 05.10.-a, 05.50.+q, 11.10.-z, 11.30.Qc, 12.38Lg]

1 Introduction

Recently spherical field theory has been introduced as a non-perturbative method for studying quantum field theory [1]. The starting point of this approach is to decompose field configurations in a d -dimensional Euclidean functional integral as linear combinations of spherical partial waves. Regarding each partial wave as a distinct field in a new one-dimensional system, the functional integral is rewritten as a time-evolution equation, with radial distance serving as the parameter of time. The core idea of spherical field theory is to reduce quantum field theory to a set of coupled quantum-mechanical systems. The technique used is partial wave decomposition, but this can easily be generalized to other modal expansions. Instead of concentric spheres and partial waves, we might instead consider a generic smooth one-parameter family of $(d-1)$ -dimensional

Support provided by the National Science Foundation under Grant 5-22698

^yemail: marrero@het.phast.umass.edu

^zemail: roura@het.phast.umass.edu

^xemail: dlee@het.phast.umass.edu

manifolds (disjoint and compact) and basis functions defined over each manifold. There are clearly many possibilities and we can optimize our expansion scheme to suit the specific problem at hand.

One important and convenient feature of spherical field theory is that it eliminates the need to compactify space | the spherical quantization surface is already compact. This is useful for studying phenomena which might be influenced by our choice of boundary conditions, such as topological excitations. Another interesting example arises in the process of quantization on noncommutative geometries. Spherical field methods have recently been adapted to study quantum field theory on the noncommutative plane [2]. In many instances, however, maintaining exact translational invariance is of greater value than non-compactness or exact rotational invariance. In that case one could consider a system whose spatial dimensions have been compactified to form a periodic box. The next step would be to expand field configurations using free modes of the box and evolve in time. We will refer to this arrangement as periodic-mode field theory or, more simply, periodic field theory.¹ The main advantage of this method is that the Hamiltonian is time independent and linear momentum is exactly conserved. In this work we describe the basic features of periodic field theory and use it to analyze spontaneous symmetry breaking in two-dimensional ⁴ theory.

The organization of this paper is as follows. We begin with a derivation of periodic field theory. We then analyze two-dimensional ⁴ theory and its corresponding periodic-field Hamiltonian using division Monte Carlo methods. We compute the critical coupling at which $\mathbb{1}$ rection symmetry is broken, and determine the critical exponents α and β . We find that our value of the critical coupling is in agreement with recent lattice results [7], and our values for the critical exponents are consistent with predictions via universality and the two-dimensional Ising model.

2 Periodic fields

We start with free scalar field theory in two dimensions subject to periodic boundary conditions

$$\langle t; L \rangle = \langle t; L \rangle : \quad (1)$$

Let J be an external source satisfying the same boundary conditions and which vanishes as $|J| \rightarrow 1$. The generating functional in the presence of J is given by

$$Z[J] / D \exp \int_1^n \int_1^{R_1} \int_L^{R_L} \int_0^h \left(\frac{1}{2} \left(\frac{\partial \phi}{\partial t} \right)^2 + \left(\frac{\partial \phi}{\partial x} \right)^2 + \frac{1}{2} J^2 \right) : \quad (2)$$

¹Periodic field theory could be viewed as a hybrid of the Hamiltonian and momentum-space lattice formalisms. This combination, however, has not been discussed in the literature.

²We are using standard notation. β is associated with the inverse correlation length, and corresponds with the behavior of the vacuum expectation value of ϕ .

We now expand in terms of periodic-box modes,

$$\begin{aligned} q \frac{1}{2L} P_{n=0, 1, \dots, n} (t) e^{in x=L} ; \\ J (t; x) = \frac{1}{2L} P_{n=0, 1, \dots, n} J_n (t) e^{in x=L} ; \end{aligned} \quad (3)$$

These are also eigenmodes of momentum and each J_n carries momentum $\frac{n}{L}$. In terms of these modes, we have

$$Z [J] / \int_0^T \prod_{n=1}^N \exp \left[\frac{1}{2} \frac{d^2}{dt^2} \frac{J_n}{L} + \frac{1}{2} \frac{n^2}{L^2} \right] + \dots \quad (4)$$

For notational purposes we will denote

$$!_n = \frac{n^2}{L^2} + \dots \quad (5)$$

Using the Feynman-Kac formula, we find

$$Z [J] / \hbar \Omega j T \exp \int_0^T dt H_J \circ \mathcal{D}i; \quad (6)$$

where

$$H_J = \frac{P}{n} \frac{h}{2} \frac{\partial}{\partial q_n} \frac{\partial}{\partial q_n} + \frac{1}{2} !_n^2 q_n q_n \quad J_n q_n; \quad (7)$$

and $\mathcal{D}i$ is the ground state of H_0 . Since H_0 is the usual equal-time Hamiltonian, $\mathcal{D}i$ is the vacuum. H_0 consists of a set of decoupled harmonic oscillators, and it is straightforward to calculate the two-point correlation functions,

$$\hbar \Omega j_n (t_2) j_n (t_1) \mathcal{D}i = \frac{1}{J_n (t_2)} \frac{1}{J_n (t_1)} Z [J]_{J=0} = \frac{1}{2 !_n} \exp [- !_n (t_2 - t_1)]; \quad (8)$$

We now include a $\frac{1}{4}$ interaction term as well as a counterterm Hamiltonian, which we denote as H_{ct} . The new Hamiltonian is

$$\begin{aligned} H_J = & \frac{P}{n} \frac{h}{2} \frac{\partial}{\partial q_n} \frac{\partial}{\partial q_n} + \frac{1}{2} !_n^2 q_n q_n \quad J_n q_n \\ & + \frac{P}{4 \Omega L} \sum_{n_1+n_2+n_3+n_4=0} q_{n_1} q_{n_2} q_{n_3} q_{n_4} + H_{\text{ct}}; \end{aligned} \quad (9)$$

We will regulate the sums over momentum modes by choosing some large positive number N_{max} and throwing out all high-momentum modes q_n such that $|n| > N_{\text{max}}$. This corresponds to a momentum cutoff

$$2 = \frac{N_{\text{max}}}{L}^2; \quad (10)$$

In two-dimensional $\frac{1}{4}$ theory, renormalization can be implemented by normal ordering the $\frac{1}{4}$ interaction term. This corresponds to cancelling diagrams of the type shown in Figure 1. Using (8), we find

$$H_{\text{ct}} = \frac{6}{4 \Omega L} \sum_{n=-N_{\text{max}}, N_{\text{max}}} q_n q_n; \quad (11)$$

where

$$b = \frac{P}{n = N_{\max} \cdot N_{\max} \frac{1}{2!_n}} : \quad (12)$$

For the remainder of our discussion we will use the Hamiltonian

$$H = H_0 = \sum_{n=1}^P \frac{h}{2} \frac{q_n}{q_{2n}} + \frac{1}{2} \left(\frac{1}{n} - \frac{b}{4L} \right) q_n q_n^i + \frac{1}{4!2L} \sum_{n_1+n_2+n_3+n_4=0} q_{n_1} q_{n_2} q_{n_3} q_{n_4} : \quad (13)$$

3 The $\frac{4}{2}$ phase transition

The existence of a second-order phase transition in two-dimensional 4 theory has been derived in the literature [3][4]. The phase transition is due to developing a non-zero expectation value and the resultant spontaneous breaking of \mathbb{Z}_2 refection symmetry. It is generally believed that this theory belongs to the same universality class as the two-dimensional Ising model and therefore shares the same critical exponents. In this section we apply periodic field methods to 4 theory in order to determine the critical coupling and critical exponents and β . We have chosen $\beta = 1$ since these are, in our opinion, the easiest to determine from direct computations. All other exponents can be derived from these using well-known scaling laws. From the Ising model predictions we expect

$$\gamma = 1; \quad \nu = \frac{1}{8} : \quad (14)$$

is the exponent associated with the inverse correlation length or, equivalently, the mass of the one-particle state. We will determine the behavior of the mass as we approach the critical point from the symmetric phase of the theory. Let $|ji\rangle$ be any state even under refection symmetry. We consider the matrix element

$$f(t) = \langle h | j_0 \exp(-tH) j_0 | j_i \rangle. \quad (15)$$

Inserting energy eigenstates $|ji\rangle$ satisfying $H|ji\rangle = E_i|ji\rangle$, we have

$$f(t) = \sum_i \exp(-tE_i) |j_i j_0|^2 |j_i j_i|^2 : \quad (16)$$

Since $|j_i\rangle$ and $|j_i\rangle$ are even under refection symmetry and j_0 is odd, the vacuum contribution to the sum in (16) vanishes. In the limit $t \rightarrow 1$, (16) is dominated by the contribution of the next lowest energy state, the one-particle state at rest.³ In this limit we have

$$f(t) \sim e^{-m t}; \quad (17)$$

³We are assuming that this contribution does not also vanish. This is generally true, and we can always vary $|j_i\rangle$ to make it so.

where m is the mass. We can compute $f(t)$ numerically using the method of diusion Monte Carlo (DMC). The idea of DMC is to model the dynamics of the imaginary-time Schrödinger equation using the diffusion and decay/production of simulated particles. The kinetic energy term in the Hamiltonian determines the diffusion rate of the particles (usually called replicas) and the potential energy term determines the local decay/production rate. A self-contained introduction to DMC can be found in [5].

is defined by the behavior of m near the critical coupling c :

$$m(c) : \quad (18)$$

Once we determine $f(t)$ using DMC simulations we can extract m and c using curve-fitting techniques. We have calculated m as a function of c for several different values of L and N_{\max} . Results from these calculations are presented in the next section.

c is the critical exponent describing the behavior of the vacuum expectation value. In the symmetric phase the vacuum state is unique and invariant under the refection transformation $! : q_n \mapsto -q_n$ (or equivalently $q_n \mapsto q_n$; for each n): In the broken-symmetry phase the vacuum is degenerate as $L \rightarrow 1$, and q_0 , the zero-momentum mode, develops a vacuum expectation value. In the $L \rightarrow 1$ limit tunnelling between vacuum states is forbidden. One ground state, $\mathcal{P}^+ i$, is non-zero only for values $q_0 > 0$ and the other, $\mathcal{P}^- i$, is non-zero only for $q_0 < 0$. We will choose $\mathcal{P}^+ i$ and $\mathcal{P}^- i$ to be unit normalized.

Let us now define the symmetric and antisymmetric combinations,

$$\begin{aligned} \mathcal{P}^s i &= \frac{1}{2} (0^+ + 0^-) \\ \mathcal{P}^a i &= \frac{1}{2} (0^+ - 0^-) : \end{aligned} \quad (19)$$

We will select the relative phases of $\mathcal{P}^- i$ and $\mathcal{P}^+ i$ so that they transform from one to the other under reflection symmetry. $\mathcal{P}^s i$ and $\mathcal{P}^a i$ are then symmetric and antisymmetric (respectively) under reflection symmetry.

To avoid notational confusion in the following, we will write q_n to denote the quantum-mechanical position operator and q_n for the corresponding ordinary variable. Let \hat{P}_z be the spectral family associated with the operator $\frac{q_0}{2L}$.⁴ This implies that \hat{P}_z is a projection operator whose action on a general wavefunction ψ is

$$\int_a^b d\hat{P}_z \psi(q_0; q_1; \dots) = \frac{q_0}{2L} \psi(a) - \frac{q_0}{2L} \psi(b) : \quad (20)$$

From the support properties of $\mathcal{P}^+ i$ and $\mathcal{P}^- i$, we deduce

$$\begin{aligned} 0^+ &= \frac{p}{2} \int_0^{R_1} d\hat{P}_z \mathcal{P}^s i = \frac{p}{2} \int_0^{R_1} d\hat{P}_z \mathcal{P}^a i \\ 0^- &= \frac{p}{2} \int_{-R_0}^0 d\hat{P}_z \mathcal{P}^s i = \frac{p}{2} \int_{-R_0}^0 d\hat{P}_z \mathcal{P}^a i : \end{aligned} \quad (21)$$

⁴The extra factor $\frac{1}{2L}$ has been included for later convenience.

Using our new spectral language, we can write

$$\hat{p}_{\frac{d_0}{2L}} = \int_1^{R_1} z d\hat{P}_z : \quad (22)$$

We now consider the vacuum expectation value $\langle 0^+ | \hat{p}^+ | 0^+ \rangle$.⁵ Making use of translational invariance, we have

$$\langle 0^+ | 0^+ \rangle = \frac{1}{2L} \int_L^{R_1} dx \langle 0^+ | (t, x) | 0^+ \rangle = \langle 0^+ | \hat{p}_{\frac{d_0}{2L}} | 0^+ \rangle : \quad (23)$$

From (21) and (22), we conclude that

$$\langle 0^+ | 0^+ \rangle = 2 \langle 0^+ | \int_0^{R_1} z d\hat{P}_z | \hat{p}^s i \rangle = 2 \int_0^{R_1} dz g(z); \quad (24)$$

where

$$g(z) = \langle 0^+ | \int_0^{R_1} z d\hat{P}_z | \hat{p}^s i \rangle : \quad (25)$$

$g(z)$ satisfies the normalization condition

$$\int_1^{R_1} dz g(z) = 2 \int_0^{R_1} dz g(z) = 1: \quad (26)$$

In our calculations we will be working with large but finite L . In this case the ground state degeneracy is not exact, and the symmetric state $\hat{p}^s i$ is slightly lower in energy than the antisymmetric state $\hat{p}^a i$. We can now use this observation (that $\hat{p}^s i$ is the lowest energy state) to rewrite $g(z)$ as

$$g(z) = \langle 0^+ | \int_0^{R_1} z d\hat{P}_z | \hat{p}^s i \rangle = \lim_{t \rightarrow 1} \frac{\langle 0^+ | \hat{p}^s i | \exp^{-tH} \int_0^{R_1} z d\hat{P}_z | \exp^{-tH} \hat{p}^s i \rangle}{\langle 0^+ | \hat{p}^s i | \exp^{-tH} \hat{p}^s i \rangle}; \quad (27)$$

where $\hat{p}i$ is any state such that $\langle 0^+ | \hat{p}i \rangle$ is non-zero.

For free field theory $g(z)$ can be exactly calculated,

$$g(z) = \frac{q}{2L} e^{-2Lz^2}: \quad (28)$$

For non-trivial coupling we can calculate the right-hand side of (27) using DMC methods. In Figure 2 we have plotted $g(z)$ for $L = 2.5$ and $L = 5$. In each case $\frac{q}{4!} = 2.76$ and $q = 4$. All quantities are measured in units where $\hbar = 1$. As can be seen, the distributions are bimodal and the maxima for both curves occur near 0.55 . We observe that the peaks are taller and narrower for larger L : This is consistent with our intuitive picture of fluctuations in the functional integral. For a small but fixed deviation in the average value of $\langle \hat{p}^s i | \hat{p}^s i \rangle$, the net change in an extensive quantity such as the action or total energy scales proportionally with the size of system. Consequently the average size of the fluctuations must decrease with L . We can estimate the amplitude of the fluctuations, $\langle \hat{p}^s i | \hat{p}^s i \rangle$, by assuming a quadratic dependence in $\langle \hat{p}^s i | \hat{p}^s i \rangle$ about the local

⁵We could also consider $\langle 0^+ | 0^+ \rangle$. By reflection symmetry $\langle 0^+ | 0^+ \rangle = \langle 0^+ | 0^+ \rangle$:

minimum. The net effect of the fluctuation should not scale with L , and we conclude that⁶

$$S = \frac{1}{L} = \frac{1}{L} : \quad (29)$$

This agrees with the free field result in (28) and also appears to be consistent with the peak widths plotted in Figure 2.

Let z_{max} be the location of the non-negative maximum of $g(z)$. Since $g(z)$ becomes sharply peaked as $L \rightarrow 1$,

$$0^+ = 2 \int_0^{R_1} dz g(z) \underset{L \rightarrow 1}{\sim} 2z_{\text{max}} \int_0^{R_1} dz g(z) = z_{\text{max}}. \quad (30)$$

This gives us another option for calculating the vacuum expectation value. We can either integrate $2zg(z)$ or read the location of the maximum point z_{max} . Both will converge to the same value as $L \rightarrow 1$. However, the z_{max} result is less prone to systematic error generated by the $O(\frac{1}{L})$ fluctuations described above.⁷ We will therefore use

$$0^+ = z_{\text{max}} : \quad (31)$$

is defined by the behavior of the vacuum expectation value as we approach the critical coupling,

$$0^+ = (\dots) : \quad (32)$$

Using DMC methods; we have computed the dependence of the vacuum expectation value for several values of L and N_{max} . The results are shown in the next section.

4 Results

The results of our division Monte Carlo simulations are presented here. For each set of parameters L and N_{max} ; the curves for m and $h0^+ j \bar{p}^+$ in near the critical coupling have been fitted using the parameterized forms

$$m = a \frac{c}{4!} \frac{h^i}{4!} : \quad (33)$$

and

$$0^+ = b \frac{c}{4!} \frac{h^i}{4!} : \quad (34)$$

⁶The dimension of time does not enter here since we are considering properties of the vacuum, the ground state of the Hamiltonian defined at a given time. This is in contrast with lattice calculations which usually consider the quantity h is, the average of h over all space and time.

⁷We can see this explicitly in free field theory, where the vacuum expectation value should vanish. $z_{\text{max}} = 0$ as desired, but $2 \int_0^{R_1} dz g(z) = \frac{1}{2} \frac{c}{L}$:

The curves for the data set $L = 2.5$ and $N_{\max} = 10$ are shown in Figures 3 and 4. As mentioned before, we are using units where $\hbar = 1$. The final results of the fits are as follows:

$L = 2.5$; $N_{\max} = 8$ ($\ell = 32$):

$$\frac{m}{4!} = 3.1; \quad = 1.0; \quad a = 0.32; \quad \frac{h_i}{4!} = 2.5; \quad = 0.15; \quad b = 0.65; \quad (35)$$

$L = 2.5$; $N_{\max} = 10$; ($\ell = 4$):

$$\frac{m}{4!} = 2.9; \quad = 1.1; \quad a = 0.35; \quad \frac{h_i}{4!} = 2.5; \quad = 0.18; \quad b = 0.70; \quad (36)$$

$L = 5$; $N_{\max} = 16$; ($\ell = 32$):

$$\frac{m}{4!} = 3.0; \quad = 1.2; \quad a = 0.33; \quad \frac{h_i}{4!} = 2.7; \quad = 0.12; \quad b = 0.62; \quad (37)$$

$L = 5$; $N_{\max} = 20$; ($\ell = 4$):

$$\frac{m}{4!} = 2.9; \quad = 1.2; \quad a = 0.35; \quad \frac{h_i}{4!} = 2.5; \quad = 0.12; \quad b = 0.65; \quad (38)$$

These results are subject to errors due to the finite size L and finite cut-off scale. We now use our data for different values of L and ℓ to extrapolate to the limit $L \rightarrow 1$; $\ell \rightarrow 1$. For the parameters m , a , b , we use the simple asymptotic form

$$x(L; \ell) = x + \frac{1}{L^2} x_{L^2} + \frac{1}{L^4} x_{L^4} + \dots \quad (39)$$

For the critical couplings $\frac{m}{c}$ and $\frac{h_i}{c}$, however, we modify the finite L correction according to the finite-size scaling hypothesis [6]

$$(L; \ell) = x + \frac{1}{L^2} x_{L^2} + \frac{1}{L^4} x_{L^4} + \dots \quad (40)$$

The results we find are

$$\frac{m}{4!} = 2.5 \quad 0.2; \quad = 1.3 \quad 0.2; \quad a = 0.40 \quad 0.03; \quad (41)$$

$$\frac{h_i}{4!} = 2.5 \quad 0.1; \quad = 0.14 \quad 0.02; \quad b = 0.72 \quad 0.04;$$

The error bounds represent our best estimates of the net error due to statistical, systematic, and extrapolation inaccuracies. In all cases statistical errors were the smallest source of error. Next in size were systematic errors arising from our choice of initial state and time step parameter in the DMC simulations. For data generated from the mass curves, the main source of error was due to extrapolation. The extrapolation error for the vacuum expectation value data was still the most significant, though considerably smaller than that for the mass calculations. This reduction is probably a result of the method used to

measure the vacuum expectation value.⁸ Our results for the critical exponents are consistent with the Ising model predictions

$$= 1; \quad = \frac{1}{8}; \quad (42)$$

The two results for the critical coupling $\frac{m}{4!}$ and $\frac{h_i}{4!}$ agree with each other as well as the recently obtained lattice result [7]⁹

$$\frac{c}{4!} = 256^{+0.02}_{-0.01}; \quad (43)$$

5 Summary

We have discussed the generalization of spherical field theory to other modal expansion methods, in particular, periodic field theory. Using periodic field methods we have analyzed two-dimensional⁴ theory and computed the critical coupling and critical exponents and associated with spontaneous breaking of \mathbb{Z}_2 reflection symmetry. Our value of the critical coupling is in agreement with a recent lattice calculation, and our values for the critical exponents are consistent with the critical exponents of the two-dimensional Ising model. This lends support to the popular belief that the two theories belong to the same universality class.

The full set of division Monte Carlo computations used in our analysis required about 30 hours on a 350 MHz PC processor. Complete codes can be obtained upon request from the authors. The required computational time appears to be dominated by the number of operations required to update the Hamiltonian, which scales as N_{max}^2 . Errors can be reduced quite substantially by using larger values of L and N_{max} and utilizing large-scale parallel processing. No less important, however, is that periodic field theory provides a simple and efficient approach to studying non-perturbative phenomena with only modest computer resources. Future studies have been planned to analyze phase transitions in other field theory models.

Acknowledgment

We are grateful to Eugene Gologich for useful advice and discussions. We also thank John Machta for comments on finite-size scaling.

References

[1] D. Lee, Phys. Lett. B 439 (1998) 85; D. Lee, Phys. Lett. B 444 (1998) 474; B. Borasoy, D. Lee, Phys. Lett. B 447 (1999) 98; D. Lee, N. Salwen, hep-th/9905077.

⁸We are referring to the result $0^+ - 0^+ = z_{\text{max}}$, which eliminates peak broadening effects for finite L . This is discussed at the end of the previous section.

⁹Critical exponents were not measured in this study.

[2] M . Chaichian, A . Demichev, P . Presnajder, hep-th/9904132.

[3] J. Glimm, A . Jaffe, Phys. Rev. D 10 (1974) 536; J. Glimm, A . Jaffe, T . Spencer, Comm. Math. Phys. 45 (1975) 203.

[4] S. Chang, Phys. Rev. D 13 (1976) 2778.

[5] I. Kosztin, B . Faber, K . Schulten, Amer. J. Phys. 64 (1996) 633.

[6] M . Fisher, M . Barber, Phys. Rev. Lett. 28, 1516 (1972).

[7] W . Loinaz, R . Willey, Phys. Rev. D 58 (1998) 076003.

F igures

Figure 1. The only divergent diagram , which can be cancelled by normal ordering.

Figure 2. Plot of $g(z)$ for $L = 25$ and $L = 5$. In each case $\frac{1}{4!} = 2.76$ and $= 4$.

Figure 3. Plot of m as a function of $\frac{1}{4!}$ for $L = 25$; $N_{\max} = 10$.

Figure 4. Plot of $h^{0+} j^- j^+$ as a function of $\frac{1}{4!}$ for $L = 25$; $N_{\max} = 10$.

Figure 1

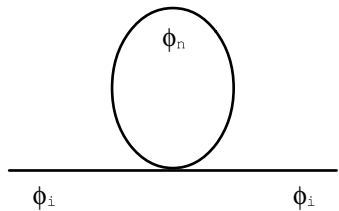


Figure 2

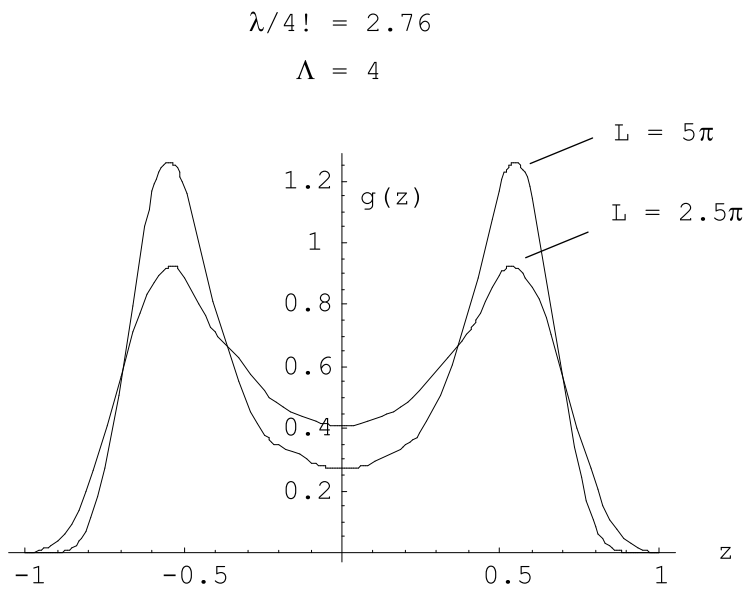


Figure 3

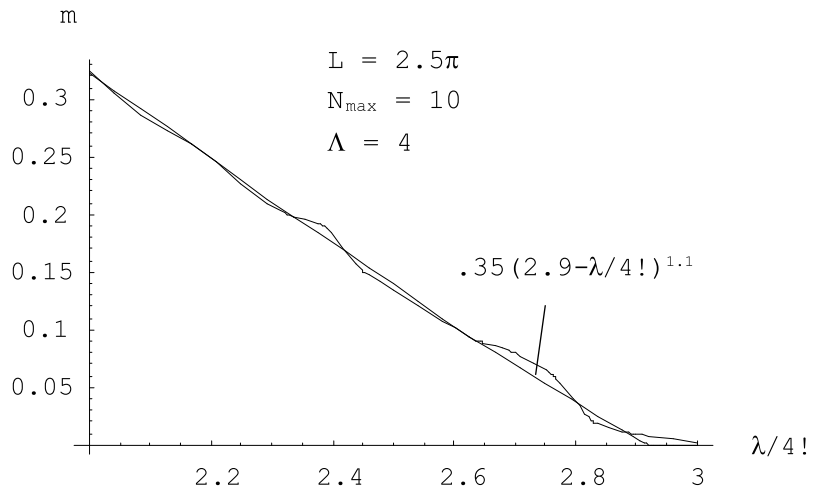


Figure 4

